*Upwelling filaments in the Benguela ecosystem, a Zooplankton-rich Oasis in the Oligotrophic Subtropical Atlantic?*

Francisco Souza Dias

Promoter & Supervisor: PD. Dr. Holger Auel

Universität Bremen

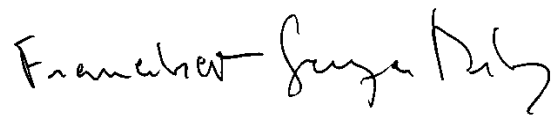Faculty of Biology and Chemistry

Department of Marine Zoology

Academic Year 2011-2012

Master thesis submitted for the partial fulfillment of the title of

**Master of Science in Marine Biodiversity and Conservation**

Within the ERASMUS MUNDUS Master Programme EMBC

## Declaration

I hereby confirm that I have independently composed this Master thesis and that no other than the indicated aid and sources have been used. This work has not been presented to any other examination board.

No data can be taken out of this work without prior approval of the thesis supervisor.

Francisco Souza Dias

Bremen, 05.06.2012

## Abstract

Upwelling filaments are narrow and long bodies of cold water protruding from an upwelling front into the warm oligotrophic ocean. The capacity for these structures to transport biomass has been studied elsewhere but a lot remains unknown in the Benguela Upwelling system. In this study, satellite imagery was used to locate the initial stage of an upwelling filament for subsequent in situ sampling of oceanographic features and zooplankton abundances and biomass inside and outside of the filament. The filament was profiled in two sections with an ADCP and CTD/XBT, Scanfish and MultiNet® were deployed. Biomass was combined with current velocity to measure inshore/offshore transport. Results show two distinct bodies of water colder than their surroundings with elevated biomass and abundances dominated by copepods in stations inside or marginal to the filament. PCA was used to assess the most remarkable taxonomic groups in each station showing that cold stations are richer in Fish eggs, small calanoids and Nauplius. Finally, biomass transport calculations revealed strong evidence for fast export offshore. Distinct taxonomic composition and elevated biomass suggests that filaments play an important ecological role in exporting biomass offshore. Further implications are discussed.

# Table of Contents

# 1. Introduction

The four major regions where coastal upwelling occurs are located within the Eastern Boundary Currents (EBCs). These are some of the most productive regions in the world. The Benguela Upwelling System belongs to one of the four EBCs. Wind blowing equator-wards combined with Coriolis force induces Ekman transport away from the coast. The low pressure generated by this transport causes for the upwell of fresher water masses from the deep ocean, naturally colder and richer in nutrients. The upwelled waters are rich in limiting nutrients that, when surfaced to the euphotic layer, fuel phytoplankton blooms that consequently feed the food web above. In fact, although EBCs cover only 1% of the ocean's surface, they account for 20% of world's fish landings (Pauly & Christensen, 1995). Despite the Benguela System productivity, consistent poor recruit years combined with enormous fishing pressure in the 1980's and 1990's has led fish stocks to a heavy decline. The Benguela is now in a depleted state; amongst the main species targeted here, were the sardine, anchovy, horse mackerel, cape hake and rock lobster (Hutchings et al., 2009; L. V. Shannon & O'Toole, 2003). The anthropogenic pressure is not limited to fishing, the Benguela system is rich in oil, gas and precious minerals that have been and will continue to be exploited in the coming years (L. V. Shannon & O'Toole, 2003).Its ecological function as well as economical relevance is thus, well established. With the development of satellite imagery (color and thermal), a new cold water structure was revealed protruding from the coastal upwelling away from the coast. Coastal upwelling was found to occur in the form of elongated "plumes" stretching over 250 km across the coast (Traganza, Conrad, & Breaker, 1981) . These structures were referred to as "upwelling filaments" as these were not floating, less dense fluids as the term "plume" suggests, but rather elongated bodies of denser cold water penetrating fast into the warm ocean with depths up to 100 m (Brink, 1983). Throughout the years, upwelling filaments have been referred to as tongues, squirts, plumes or jets. A simple way to define an upwelling filament is as a narrow protuberance extending more than 50 km from the upwelling front whenever the ratio of length to width exceeds two (L/D > 2 where L and D are the length and width of the filament, respectively) (Kostianoy & Zatsepin, 1996). A number of studies have addressed the physical structure, and transport of nutrients, biomass, and suspended matter of upwelling filaments especially off the coasts of California

and Northwest Africa ((Alvarez-Salgado et al., 2001; Flament & Washburn, 1985; Rodriguez, Hernandezleon, & Barton, 1999). In comparison, much less is known about the upwelling filaments of the Benguela system. Remarkably, despite their established biological and chemical roles, the physical processes that generate upwelling filaments are still not entirely disclosed. Several mechanisms through which filaments might be generated have been proposed for upwelling filaments, often with interaction of capes (Nelson, Boyd, & Agenbag, 1998; Strub, Kosro, & Huyer, 1991) more recently, that wind in combination with topography is the key for generating an upwelling filament, at least in Cape Ghir, in Northwest African coast (Charles Troupin, Mason, Beckers, & Sangrà, 2012). In addition, filaments are known to frequently change their dynamics; splitting their main core, changing direction and terminating in eddy-like structures (Lutjeharms, Shillington, & Rae, 1991; Strub et al., 1991). Moreover, filaments residence time varies depending on the strength of upwelling-favorable winds, turbulence and other factors as the filament warms and downwells into the blue ocean(Haynes, Barton, & Lino, 1993). Upwelling filaments are narrow bodies of cold water protruding from the upwelling front with the ability to change transport dynamics in the surrounding areas. It has been showed that productivity is increased inside the filament (Shelton & Hutchings, 1990)while other studies point in the opposite direction (Shillington et al., 1990). Similarly, the distinct characteristics of the filament have been suggested to act as a barrier to faunal movement across it with evidence supporting the effectiveness of this barrier in California(Keister, Di Lorenzo, Morgan, Combes, & Peterson, 2011) and Canary Islands (Hernández-León, Gómez, & Arístegui, 2007). In the first description of the biological composition of an upwelling filament in the Benguela system it was reported depleted biodiversity when compared to the upwelling front, describing a filament rich in salps which was attributed to the decaying state of the filament as it was sampled towards its final stage(Shillington et al., 1990). The frequency and characteristics of upwelling filaments in the Benguela system has been described as (a) the concentration of filaments is higher in the region 18°-19°, 22°-23°30', 26°-27°30'S than elsewhere in the Benguela System; (b) filaments propagate perpendicularly from the upwelling front; (c) filaments are carried out from the coast to a distance of 500 to 600 km; and (d) the filaments constitute half of all Ekman transport, resulting in an export of particles from the coast to the oligotrophic

ocean (Kostianoy & Zatsepin, 1996). Without any data about the biomass carried inside the filaments, the true ecological importance of the upwelling filaments is unknown. Very little information is available on the biological composition of an upwelling filament. In a study of the ichthyoplanktonic community of an upwelling filament off Northwest Africa, it was reported that 94% of neritic larvae were captured in oceanic waters inside the filament, while oceanic larvae were strongly excluded from it (Rodriguez et al., 1999). Elevated zooplankton biomass was also encountered offshore whenever advective structures were present, without, however, any further information regarding the species composition (Keister, Cowles, Peterson, & Morgan, 2009). Nevertheless, the faunal distribution has been compared between distinct water bodies of different temperatures in the Angola Benguela Front (other than filaments) with different preferences amongst copepod species (Loick & Ekau, 2005). These studies not only point towards an important transport of biomass associated with upwelling filaments, but also to differences in species composition within them. Still, it remains unclear the true effect of filaments in the biogeographic distribution of zooplankton and their role in the transport of biomass inshore and offshore. "Benguela Niños", a phenomenon first coined by Shannon (L. Shannon, Boyd, & Brundrit, 1986), refers to decadal incursions of warm water into the upwelling zone associated with weakening of upwelling-favorable winds. This brings primary productivity to a halt, starving the trophic levels above. Since upwelling filaments are dependent on the strength of the upwelling front where they originate and both Climate Change and Benguela Niños may have an impact on the strength and dimension of upwelling areas, it is likely that these phenomena may affect the frequency of upwelling filaments and their ecological function. As it is expected that filaments play an important role exporting biomass into the oligotrophic ocean, changes in this transport may escalade to higher trophic levels with impacts for commercially exploited species.

## 1.1 Aims & Hypotheses

The present study aims to answer two main questions 1) what are the abundances and biomass of zooplankton in an upwelling filament in the Benguela System? and 2) how do the transport dynamics of zooplankton biomass behaves in an upwelling

filament and its surrounding waters in the Benguela system? In particular, the following hypothesis will be tested:

$H_1$: Upwelling filaments hold higher abundances and biomass, yet lower biodiversity of zooplankton than their adjacent waters.

$H_2$: Upwelling filaments act as a vehicle for fast export of biomass from the coastal upwelling front into the warm oligotrophic ocean.

## 2. Methods and Materials

### 2.1 Study Area

This study was conducted in the northern Benguela upwelling system off the coast of Cape Frio, in Namibia. The Benguela current is driven by the South-East trade winds which blow perennially along the coast line forced by the South Atlantic Anticyclone (SAA) high pressure (Hutchings et al., 2009). The upwelling off the coast of Namibia is unique in the way that it belongs to the only EBC bordered by warm waters both to the north and the south. To the south, the Agulhas Current brings the warm waters of the Indian Ocean, and to the north the tropical waters brought by the South Equatorial Counter Current collide with the cold upwelled waters forming the Angola Benguela Front (ABF). The ABF is defined by the SST 20°C isotherm and fluctuates in its latitude over the year. The shape of the continental shelf along with its bathymetry combined with the oceanographic and atmospheric features create, at points, extremely powerful upwelling events, namely, off Cape Frio and Lüderitz. As a result of strong upwelling forcing, primary and secondary productivity are very high. The different features defining the Benguela upwelling system are shown in Figure 1 below.
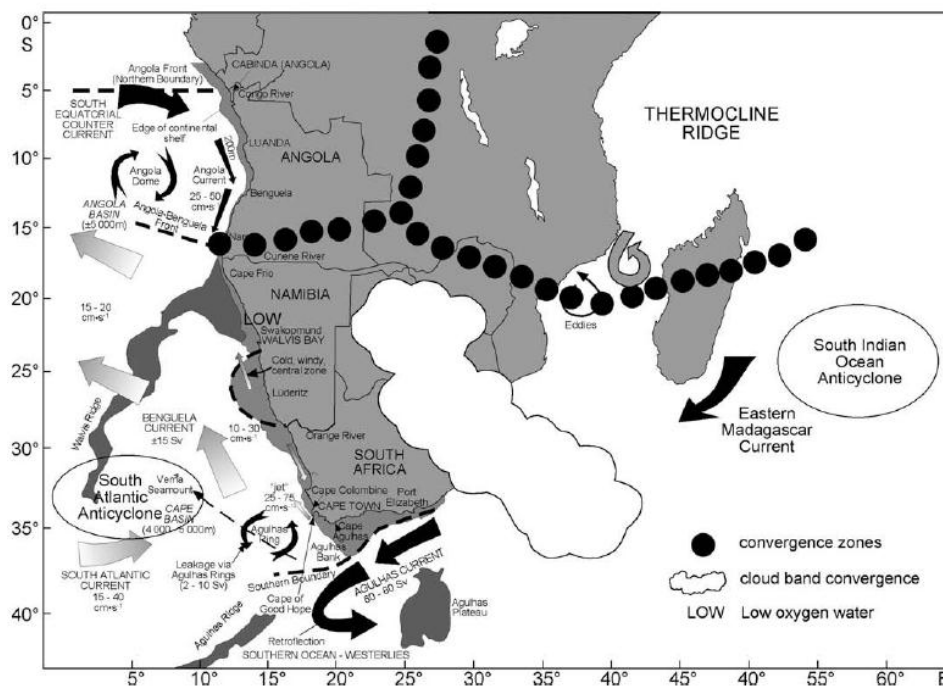


*Figure 1: Large Marine Ecosystem of Benguela* (L. V. Shannon & O'Toole, 2003)*modified by* (Hutchings et al., 2009)

## 2.2 Sampling

The samples used in this thesis were collected during leg two of the cruise for the project 'Geochemistry and Ecology of the Namibian Upwelling System' (GENUS) aboard the R.R.S. Discovery during the austral spring (1st - 5th October 2010). Data was gathered discretely at five stations and continuously along three transects as shown in Figure 2.
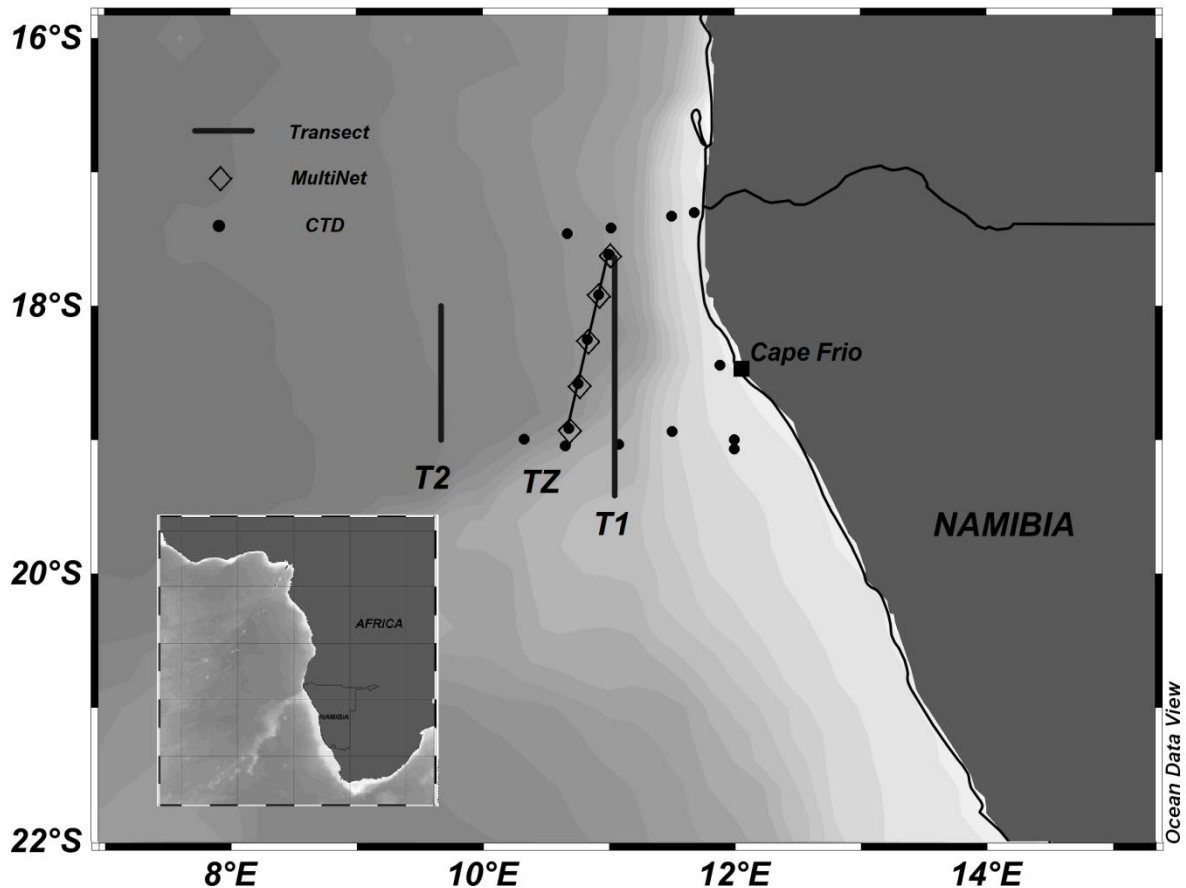


*Figure 2: Location of Transects 1, Transect 2 & Transect Z and Stations 1 to 5.*

The position of the transects was determined upon observation of satellite-acquired SST imagery (advanced very high resolution radiometer - AVHRR) transmitted to the vessel on location. The image was captured ten days before sampling commenced and showed the initial development of the filament represented by SST of ~16°C, position 18.25°S, 011.00°E and protruding half a degree offshore as indicated by the red arrow in Figure 3. No further SST-satellite images could be obtained during the sampling due to cloud coverage. Instead, the filament was tracked using Optimum

interpolated SST data from the Tropical Rainfall Measuring Mission Microwave Imager (TMI) and Advanced Microwave Scanning Radiometer for Earth Observing System (AMSR-E) as shown in Figure 4. The five zooplankton sampling stations and the transect connecting them (TZ) were positioned across the filament so as to collect samples at one station inside, two outside and two bordering the filament (Table 1). Transect 1 (T1) was similarly placed across the filament and Transect 2 (T2) was positioned parallel to and 140km west of T1. CTD was deployed in 11 additional stations to map the surrounding temperature.
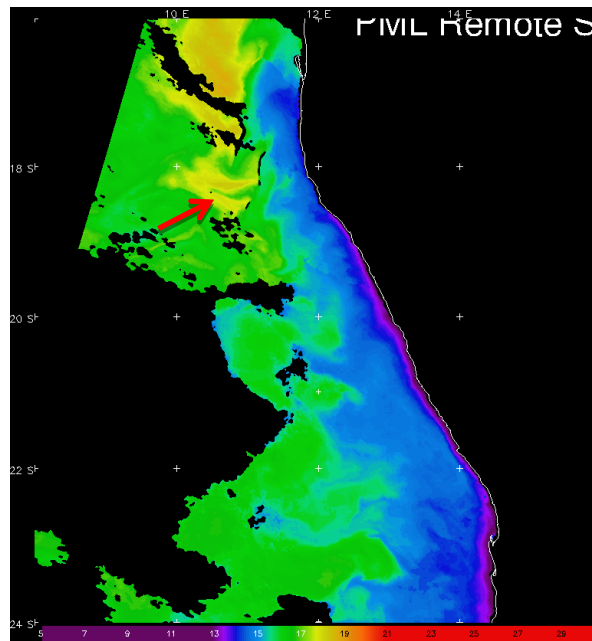


*Figure 3: Satellite-acquired SST imagery (AVHRR) showing the initial development of the filament as indicated by the red arrow*

The sampling consisted of three runs as follows: the first, a pole-wards run along T1 (1st October), the second, an equator-wards run along TZ (1st - 3rd October) and the third, a pole-wards run along transect T2 (4th October).
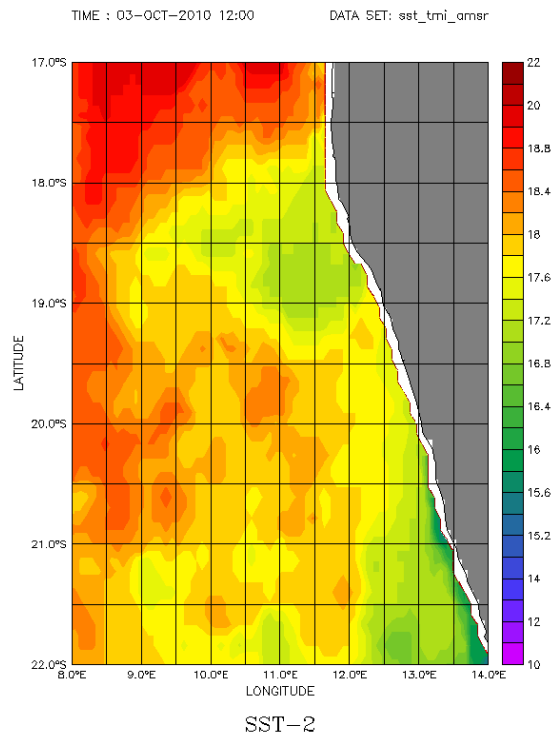
*Figure 4: Optimum interpolated SST data from the Tropical Rainfall Measuring Mission Microwave Imager (TMI) and Advanced Microwave Scanning Radiometer for Earth Observing System (AMSR-E)*

Oceanographic samples were collected across the filament in all three runs. During the first (T1) and third (T2) runs an undulating CTD (Fishscan) was towed to generate a profile of the structure of the filament. In the second run, along TZ, a vessel-mounted ADCP recorded the current velocity and direction. In addition, at each station along TZ a vertical CTD (model Seabird Electronics SBE 911 Plus) and a MultiNet® (Hydro-Bios MultiNet Type Midi, 0.25m$^2$ mouth opening, 200µm mesh size and five nets) were deployed.

Zooplankton samples were collected using a MultiNet® equipped with two electronic flow meters, on either side of the sampling frame, to record the filtered volume of water. Net 1 collected from 200 to 150m; Net 2 from 150 to 100m; Net 3 from 100 to 50m; Net 4 from 50 to 30m; Net 5 from 30m to the surface. Samples were preserved with a 4% formaldehyde-seawater solution and stored for posterior analysis.

| Station | Sample | Remark | LAT | LON | Time UTC | Depth Layers (m) | Net |
|---------|--------|--------|-----|-----|----------|------------------|-----|
| 1 | 1 | Outside of the filament (North) | 17°36.43' | 11°00.34' | 22:11 | 200-150 | 1 |
|   | 2 |  |  |  |  | 150-100 | 2 |
|   | 3 |  |  |  |  | 100-50 | 3 |
|   | 4 |  |  |  |  | 50-30 | 4 |
|   | 5 |  |  |  |  | 30-0 | 5 |
| 2 | 6 | Northern margin of the filament | 17°55.14' | 11°56.11' | 05:48 | 200-150 | 1 |
|   | 7 |  |  |  |  | 150-100 | 2 |
|   | 8 |  |  |  |  | 100-50 | 3 |
|   | 9 |  |  |  |  | 50-30 | 4 |
|   | 10 |  |  |  |  | 30-0 | 5 |
| 3 | 11 | Center of the filament | 18°16.12' | 10°49.35' | 13:18 | 200-150 | 1 |
|   | 12 |  |  |  |  | 150-100 | 2 |
|   | 13 |  |  |  |  | 100-50 | 3 |
|   | 14 |  |  |  |  | 50-30 | 4 |
|   | 15 |  |  |  |  | 30-0 | 5 |
| 4 | 16 | Southern margin of the filament | 18°35.38' | 10°46.21' | 21:54 | 200-150 | 1 |
|   | 17 |  |  |  |  | 150-100 | 2 |
|   | 18 |  |  |  |  | 100-50 | 3 |
|   | 19 |  |  |  |  | 50-30 | 4 |
|   | 20 |  |  |  |  | 30-0 | 5 |
| 5 | 21 | Outside of the filament (South) | 18°54.04' | 10°42.31' | 05:34 | 200-150 | 1 |
|   | 22 |  |  |  |  | 150-100 | 2 |
|   | 23 |  |  |  |  | 100-50 | 3 |
|   | 24 |  |  |  |  | 50-30 | 4 |
|   | 25 |  |  |  |  | 30-0 | 5 |

## Stable Isotopes

In addition to the sampling mentioned before, stable isotope analysis was conducted on selected copepod individuals. These were collected from oblique MultiNet® samples taken aboard R/V Maria S. Merian during another GENUS cruise, leg two in October of 2011. The individuals were selected from 8 stations, 3 onshore and 5 offshore (Figure 5).
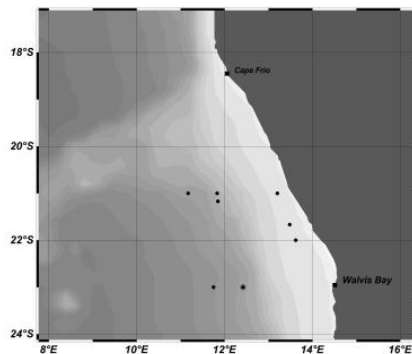


*Figure 5: Copepod sampling stations for stable isotope analysis.*

## 2.3 Analysis

XBT/CTD and Scanfish data were combined to plot a precise record of the temperature profile across the filament. (Data from Muller, Mohrholz, & Schmidt (under submission for publication))

Zooplankton samples were fractioned using a Motodo Plankton Splitter (MOTODA, 1959) with 30 mixing cycles before splitting. Fractioning was conducted until the sub-samples were diluted enough to be processed, reserving ½ subsample aside for future reference. Hence, per sample it was obtained a dilution series of sub-samples (e.g. ½ ¼ ⅛…). Analysis was performed under a high-resolution stereomicroscope Leica MZ 12-5 starting, for each sample, with the sub-sample of highest dilution and counting all organisms in each taxon. Counting continued through the following subsamples from highest to lowest dilution and zooplankton was recorded until it amounted to 50 individuals or the sample was finished and the corresponding fraction was registered. This way not only abundant taxa were counted but also the rarest ones. Abundances per station were calculated by computing the weighted average of the counts (c) using the registered volume of water by MultiNet flow meter (V) in each stratum (n).

$$\text{Abundance}_c = \frac{\frac{c_1}{V_1} + \frac{c_2}{V_2} + \frac{c_3}{V_3} + \frac{c_4}{V_4} + \frac{c_5}{V_5}}{\sum V}$$

Software Primer 6.1.10 was used to perform Principal Components Analysis (PCA) and Cluster analysis. These were conducted after transforming the abundances data using Log (x+1) in order to reduce the range of values (Clarke & Warwick, 1994). Diversity Indices were calculated using Biodiversity Professional 2.0 software.

Individual zooplankton biomass was obtained by drying (at $60^{\circ C}$ for 48h) pooled individuals of the same taxon and then calculating the average dry mass per individual. Biomass was calculated for the most abundant taxa, except for those whose individual dimensions varied significantly. Individual biomass was either estimated or based in referenced dry weight for specific taxa.

ADCP data was processed/calculated by Muller et al. (under submission for publication).

The output data from the ADCP was merged online with corresponding navigation data from the GPS output and additional heading information was provided by a gyro-compass. Post-processing of the VMADCP data was carried out using the Matlab® ADCP toolbox of IOW. The final profiles are 300s averages of the single ping profiles.

Finally, biomass transport was calculated In each station and per stratum, current velocity values were multiplied by the corresponding value of biomass. The values of biomass transport per stratum were then integrated over the considered water column (30 to 100) and expressed in $(\mu g.m^{-3})(m.s^{-1})$

## Stable Isotopes

Selected copepods for isotopic analysis were freeze-dried for 48h. Individuals in excess of adequate biomass for analysis (0.5 to 7 mg) were ground and split through multiple samples. Likewise, individuals with insufficient biomass were pooled together in order to obtain the necessary minimum weight. Samples were collected in tin capsules and the stable isotopes analysis was performed by Agroisolag GmbH in Jülich, Germany, using a mass spectrometer (EANA1500 Series 2, Carlo Erba Instruments) with helium as the carrier gas.

In order to avoid biased results, stable isotopes analysis was performed without any lipid extraction (Mintenbeck et al. 2008). The determination of Carbon and Nitrogen content was based on IAEA-VPDB (IAEA-C1) and atmospheric air (IAEA-N1), respectively, and isotopic ratios are expressed as $\delta^{13}C$ and $\delta^{15}N$ in per mil ‰, according to the equation given by Hobson et al. (2002).

Trophic Level (TL) calculation requires the estimation of a $\delta^{15}N_{base}$ (base line) value, i.e., the $\delta^{15}N$ value of an organism of known trophic level must be found. In this study, the organism used was phytoplankton (TL = 1). The $\delta^{15}N_{base}$ for phytoplankton in the Benguela system was calculated by Schukat. (unpublished), based on the mean value of two sampling transects in the Benguela System ($\delta^{15}N_{base}$ = 1.7‰).

Trophic Level was obtained through the following equation:

Trophic level = $\lambda + (\delta^{15}N_{consumer} - \delta^{15}N_{base})/3.4‰$

Where $\lambda$ is the corresponding trophic level of the organism used for $\delta^{15}N_{base}$ and 3.4‰ is the per mil value of $\delta^{15}N$ enrichment per trophic level (Hobson & Welch 1992).

## 3. Results

The results of the sample processing and basic observations of this data are presented in this section. The location of the five biological stations is shown in Figure 2. As discussed previously, the position of each station was based on the expected advecting path of the upwelling filament. The temperature map in Figure 6 (SST ODV) was generated from the CTD data at each station along with the additional 11 stations surrounding the transect using Ocean Data View software package with Data-Interpolating Variational Analysis (DIVA) (C Troupin et al., 2010) and shows temperatures as low as 13.84°C close to the shore off Cape Frio rising up to 20°C to the north. The SST within the biological stations varies from 15.26°C to 16.77°C.
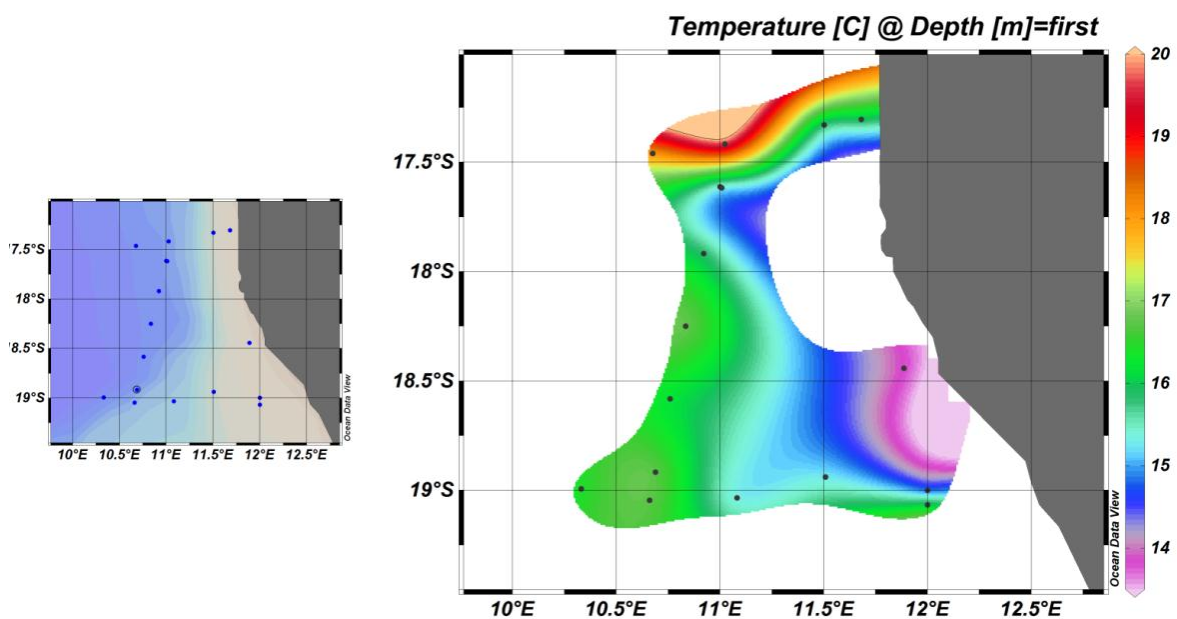


Figure 6: CTD Temperature map

Scanfish data, plotted in Figure 7, shows the temperature and salinity profiles taken across the filament in T1 and T2. The T1 profile exhibits two distinct bodies of cold water at around -18.30° and -17.65°, with a temperature anomaly of 0.5°C. T2 profile captured one single filament core.
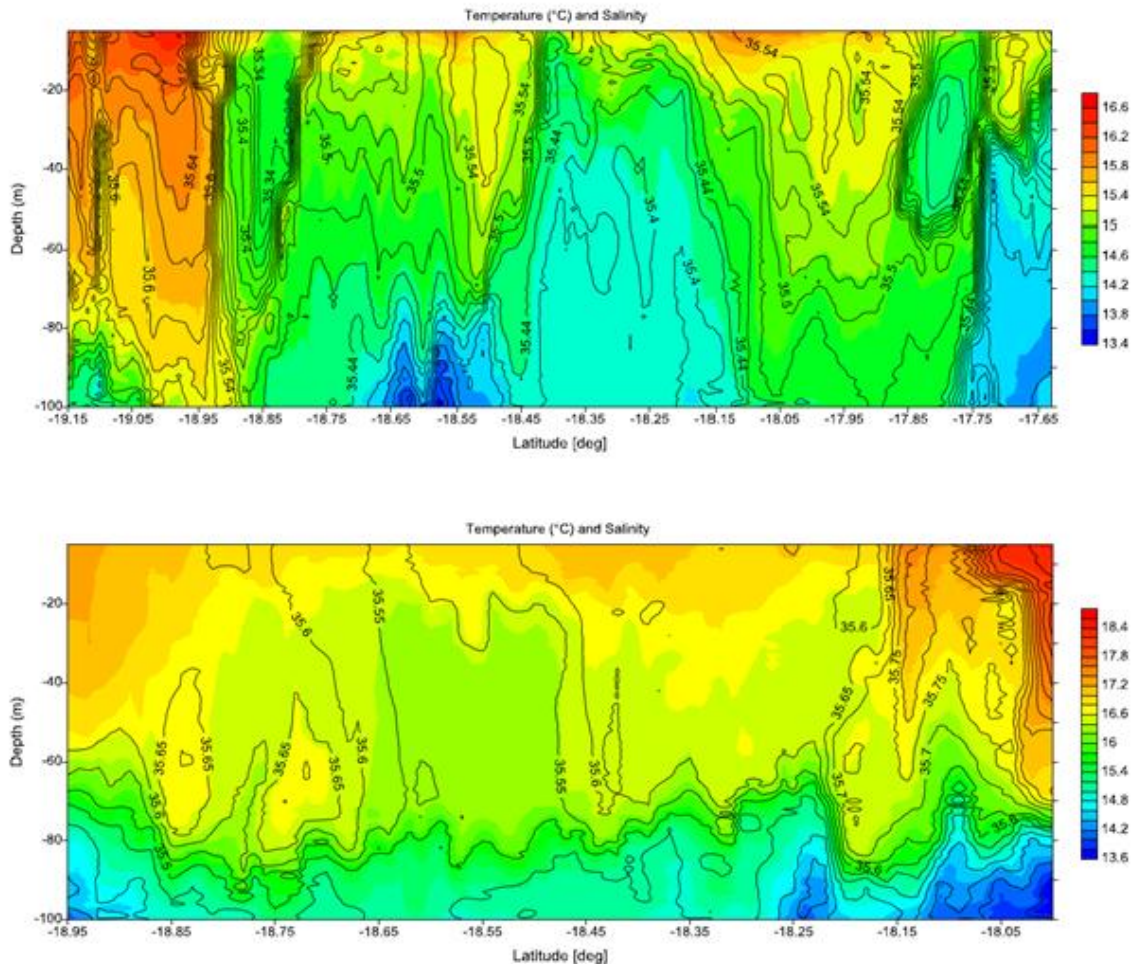


*Figure 7: Top figure shows the temperature profile for T1 and bottom figure shows temperature profile for T2. Temperature is shown in colour and isohalines in black lines.*(Muller et al., n.d.)

Two reference stations, one to the north (N) and one to the south (S) of the sampling sites were used and are shown along with the five biological stations in Figure 8. Figure 8 also shows the temperature over depth of the five sample stations as well as the two references stations over a depth of 150 meters taken from the CTD data at each site. In this map it can be seen that Station N exhibits a warm ($\simeq$ 20°C) surface layer down to around 40m depth, after which there is a sharp decline of more than 4°C, consistent with a thermocline. Stations 1, 2, and 4 are positioned southwards to Station N. It is observed that Station 1 has the coldest sea surface temperature followed by Stations 2 and 4. These show the lowest temperatures

recorded amongst all the stations and have similar profiles demonstrating a very shallow and weak thermocline converging towards 14°C. Stations 3 and 5 are warmer at the surface (16.5°C), declining after 30m, though Station 3 presents one thermocline at 25m and then another one at 80m. Station S, immediately southwards to Station 5 behaves much like it. All stations converge to approximate values of temperature as they reach the 80m depth mark.
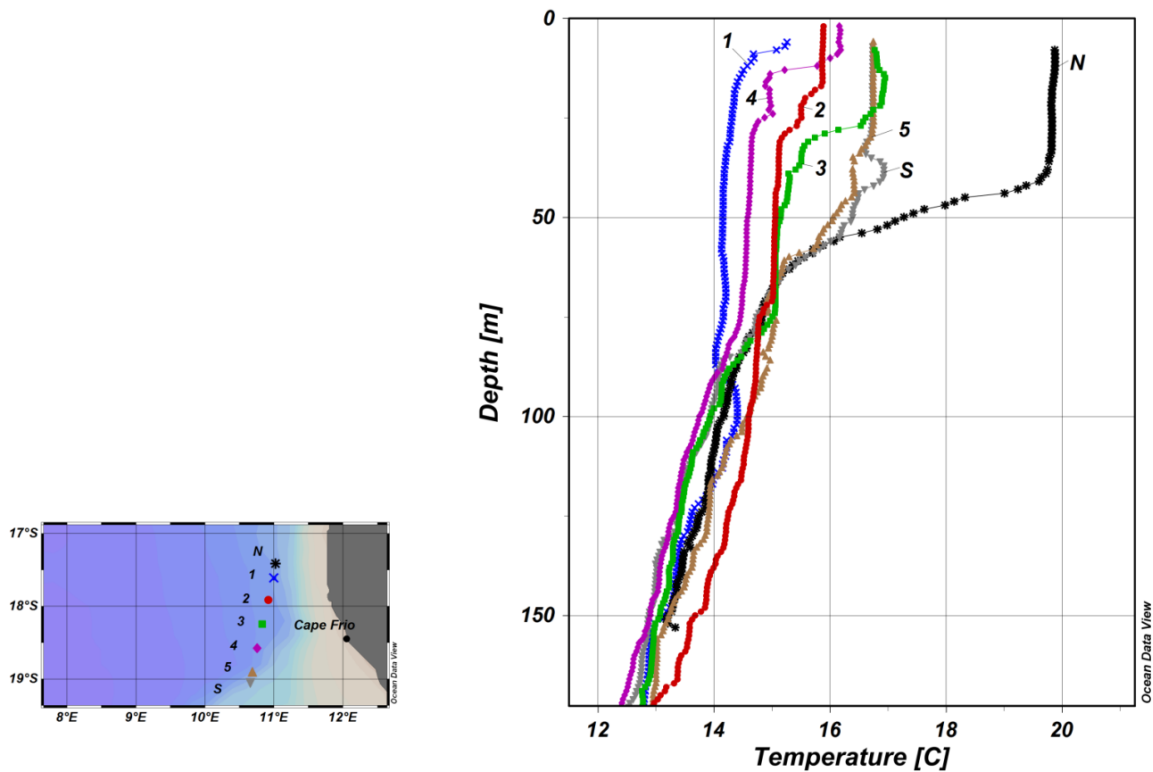


*Figure 8: Location of five biological sampling stations and two reference stations N and S (left) and temperature profile of each station over a depth of 200m (right)*

As an initial exploratory analysis of the biological data, abundances were plotted by calculating the average number of particles per cubic meter (no./m$^3$) per station as well as the contribution of each taxon in percentage. Results are presented in Figure 9. The graph on the left shows stacked average abundances per station. It can be seen that Station 2 holds the highest abundance of zooplankton amounting to approximately 722 no./m$^3$, followed by Station 1 with 304 no./m$^3$, Station 4 with 184 no./m$^3$, Station 5 with 111 no./m$^3$, and Station 3 bearing the lowest abundance with 54 no./m$^3$. The graph shown on the right illustrates the percentage of each taxon per station. It is clear that Station 2 holds the highest number of particles and the major contributor to this station is the large number of 'Fish eggs' (446 no./m$^3$; 61.8%).
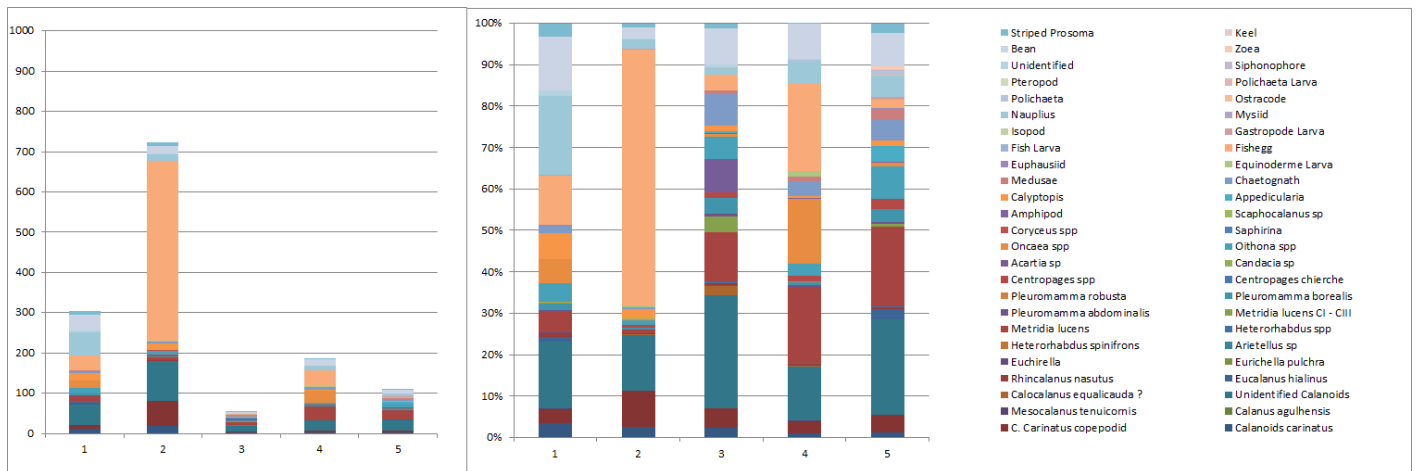
*Figure 9: Stacked average abundances of each taxon (no./m³) for each station (left) and the percentage abundance for each station (right)*

Additional information on the number of particles per station is provided in Figure 10. Here the number of particles integrated over the 200m water column is shown.
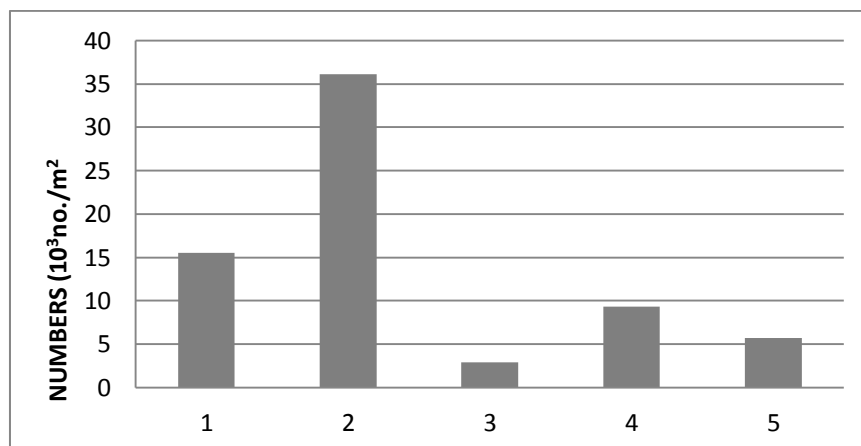


*Figure 10: Horizontal zooplankton distribution for each station*

In order to better visualize less dominant taxon and to gain a stratified vertical taxonomic composition over the water column in each station, the 'Fish egg' taxa was plotted aside (Figure 11) and the remaining taxon were plotted as above and displayed in Figure 12. Figure 11 depicts the vertical distribution of fish eggs in Station 2 showing that the majority of 'Fish eggs' are located in the surface layer of the water column from 0 to 30m. The species, to which the large number of fish eggs belongs, could not be identified. The 8 fish larvae collected were only found in Stations 1 and 2. These were identified as two Cape horse mackerel (*Trachurus trachurus capensis*) and two unidentified yolk-sack larvae in Station 1, and

18

one Southern African anchovy (*Engraulis capensis*) and three other larvae probably belonging to the sparidae family in Station 2.
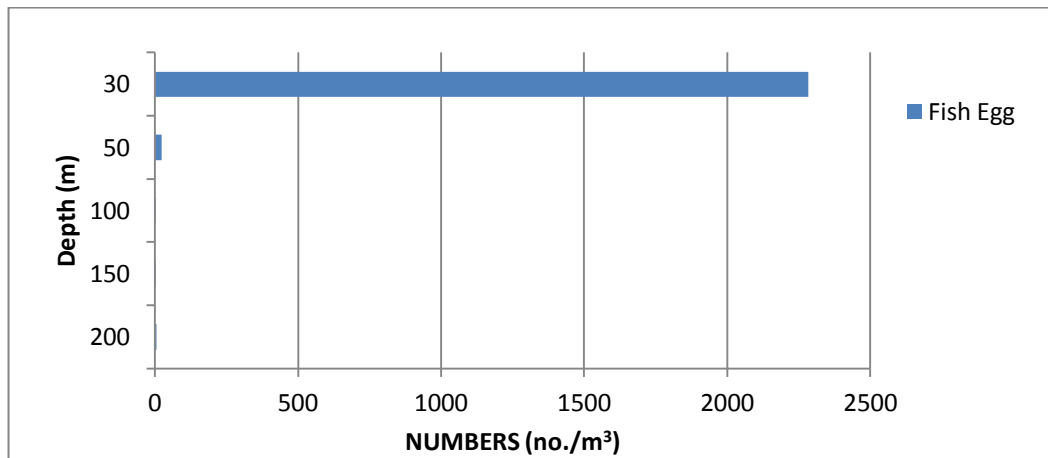


*Figure 11: Vertical distribution of Fish Egg particles in Station 2 over 200m water column*

The vertical distribution per station without the 'Fish Egg' data is represented in Figure 11 Stations 1, 2, and 4 present a fairly similar profile of decreasing number of particles per strata, though Station 4 holds a considerably lower overall number of particles. These three stations have the highest abundances at the surface layer (0 to 30m) with lower numbers in the following strata, showing a decreasing trend of abundance with depth. Stations 3 and 5 have similar profiles to each other but vary significantly from those shown in Stations 1, 2, and 4. Here the maximum abundance is also present at the surface layer (0 to 30m) yet the following stratum (30 to 50m) holds the minimum abundances after which the number of particles increases slightly as the depth increases. The taxonomic composition varies between stations and depths. Nevertheless, there are taxa common to all the stations of which high abundance is transversal to all stations. Examples include taxa *Unidentified Calanoids I* in dark blue, *Unidentified Copepods 1* in light pink, *Metridia lucens* in brown, and *Nauplius larva* in purple. Table 2 shows the weighted mean for each taxon at each of the five stations. As can be seen in Figure 9 the "Fish egg" abundances are much higher in Stations 1, 2, and 4 compared to Stations 3 and 5. In addition, it can be observed that the only taxon more predominant in Station 3 than in any other is *Acartia sp.*
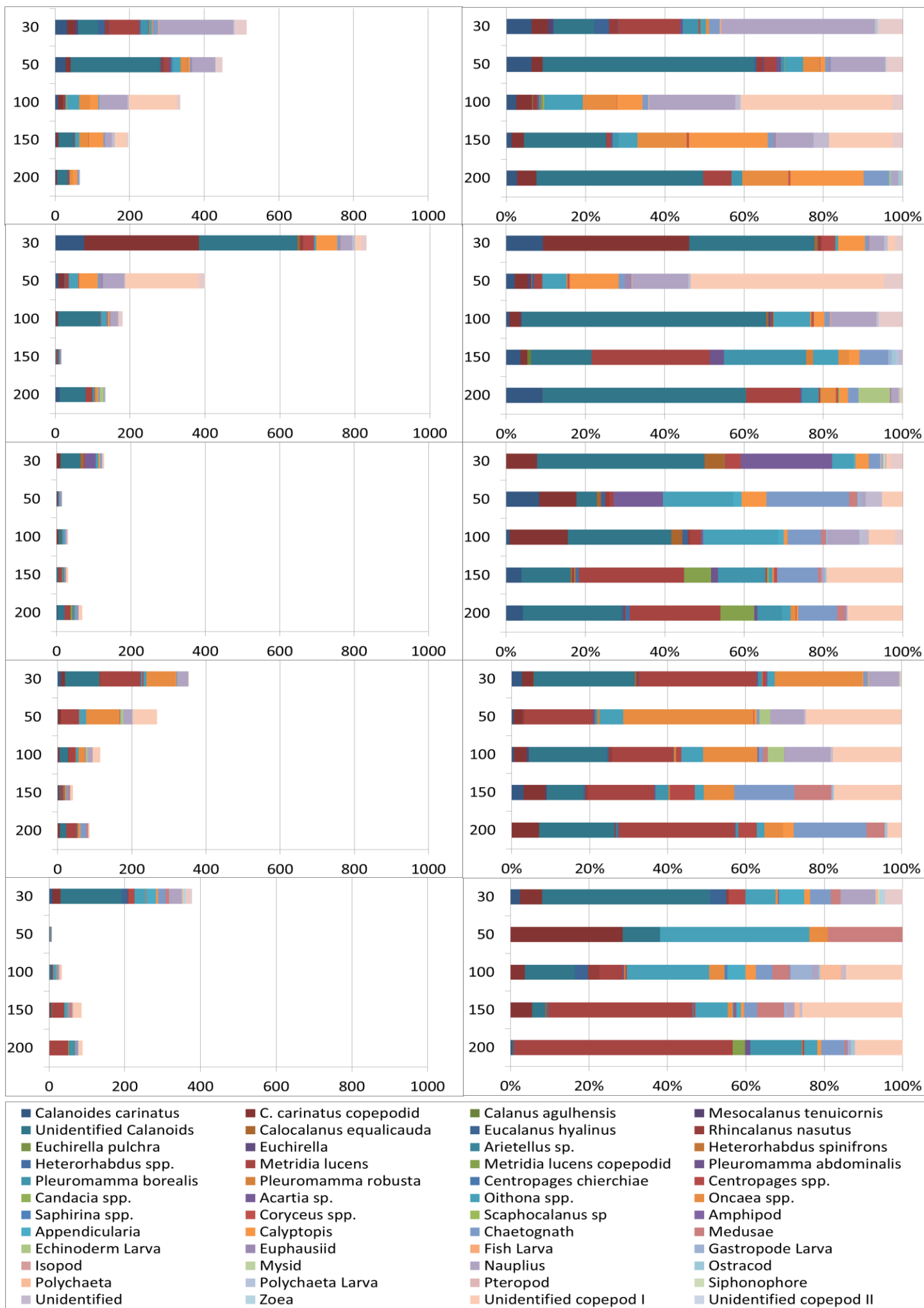
19

Figure 12: Vertical distribution of all taxa (excluding Fish Egg) showing the stacked average abundance (left) and percentage contribution (right) for Station 1 (top) to Station 5 (bottom)

*Table 2: Abundance per station and Individual Dry Weight  (a =  (Schukat, unpublished); b = estimated; c = (Huggett, 2009)*

| Order | Family | Species / Taxa | DW/ind [µg] | | Station Number | | | | |
|-------|--------|----------------|-------------|---|---|---|---|---|---|
| | | | | | 1 | 2 | 3 | 4 | 5 |
| | | | | | Mean | | | | |
| Calanoida | Calanidae | *Calanoides carinatus* | 128 | a | 14.73 | 19.97 | 1.13 | 2.50 | 1.92 |
| | | *C. carinatus copepodid* | 128 | a | 11.28 | 65.10 | 3.16 | 5.71 | 5.83 |
| | | *Calanus agulhensis* | | | 0.00 | 0.03 | 0.00 | 0.05 | 0.02 |
| | | *Mesocalanus tenuicornis* | | | 1.42 | 0.79 | 0.00 | 0.18 | 0.00 |
| | Paracalanidae | *Calocalanus equalicauda* | | | 0.16 | 1.77 | 1.48 | 0.20 | 0.06 |
| | Eucalanidae | *Eucalanus hyalinus* | 748 | a | 4.31 | 0.58 | 0.20 | 0.17 | 3.36 |
| | | *Rhincalanus nasutus* | 516 | a | 4.32 | 1.75 | 0.14 | 1.07 | 0.65 |
| | Aetideidae | *Euchirella pulchra* | 453 | a | 0.00 | 0.00 | 0.05 | 0.00 | 0.00 |
| | | *Euchirella* | 1086 | a | 0.27 | 0.00 | 0.00 | 0.00 | 0.00 |
| | Arietellidae | *Arietellus sp* | 745 | a | 0.00 | 0.00 | 0.00 | 0.03 | 0.00 |
| | Heterorhaddidae | *Heterorhabdus spinifrons* | | | 0.00 | 0.00 | 0.03 | 0.00 | 0.00 |
| | | *Heterorhabdus spp* | | | 0.14 | 0.15 | 0.21 | 0.14 | 0.10 |
| | Metridinidae | *Metridia lucens* | 60 | a | 20.46 | 6.15 | 5.00 | 40.81 | 16.61 |
| | | *Metridia lucens CI - CIII* | 22 | a | 0.00 | 0.00 | 1.60 | 0.00 | 0.56 |
| | | *Pleuromamma abdominalis* | 60 | a | 1.98 | 0.23 | 0.21 | 0.64 | 0.29 |
| | | *Pleuromamma borealis* | 325 | a | 5.97 | 1.90 | 1.60 | 1.47 | 2.35 |
| | | *Pleuromamma robusta* | 325 | a | 0.16 | 0.06 | 0.00 | 0.60 | 0.06 |
| | Centropagidae | *Centropages chierchiae* | 60 | a | 0.13 | 0.00 | 0.00 | 0.00 | 0.00 |
| | | *Centropages spp* | 60 | a | 0.50 | 5.99 | 1.08 | 2.28 | 3.39 |
| | Candaciidae | *Candacia sp* | 202 | a | 0.54 | 0.05 | 0.03 | 0.00 | 0.00 |
| | Acartiidae | *Acartia sp* | 74 | a | 0.00 | 0.00 | **6.30** | 0.20 | 0.00 |
| | Oithonidae | *Oithona spp* | 20 | a | 13.87 | 9.43 | 3.36 | 6.37 | 9.72 |
| | Oncaeidae | *Oncaea spp* | 20 | a | 16.88 | 1.56 | 0.21 | 38.42 | 1.04 |
| | Sapphirinidae | *Saphirina* | | | 0.00 | 0.00 | 0.00 | 0.00 | 0.10 |
| | Corycaeidae | *Coryceus spp* | 30 | c | 0.32 | 0.78 | 0.08 | 0.11 | 0.03 |
| | Scolecitrichidae | *Scaphocalanus sp* | | | 0.00 | 0.11 | 0.00 | 0.00 | 0.00 |
| | Unindentified Copepodes | *Unidentiied Copepod I* | | | 31.89 | 42.31 | 3.97 | 19.24 | 7.54 |
| | | *Unidentified Copepod II* | | | 0.00 | 0.08 | 0.00 | 0.00 | 0.00 |
| | | *Unidentified Copepod III* | 17 | b | 12.95 | 8.81 | 0.86 | 0.15 | 3.44 |
| | | *Unidentified Calanoids* | 17 | c | 72.32 | 88.95 | 16.71 | 27.11 | 33.89 |
| Amphipoda | | *Amphipod* | | | 0.07 | 0.00 | 0.00 | 0.09 | 0.22 |
| | | *Appendicularia* | | | 0.00 | 0.00 | 0.30 | 0.00 | 5.39 |
| Euphausiacea | | *Calyptopis* | 18 | b | 15.69 | 22.72 | 1.15 | 1.05 | 1.62 |
| | | *Euphausiid* | | | 0.40 | 1.99 | 0.03 | 0.03 | 0.08 |
| | | *Chaetognath* | | | 5.99 | 3.97 | 3.88 | 5.75 | 5.90 |
| | | *Medusae* | | | 0.21 | 0.15 | 0.45 | 2.00 | 3.67 |
| | | *Echinoderm Larva* | | | 0.10 | 2.11 | 0.00 | 2.62 | 0.00 |
| | | *Fishegg* | 45 | b | 58.49 | 463.1 | 1.89 | 51.93 | 2.92 |
| | | *Fish Larva* | | | 0.46 | 0.19 | 0.00 | 0.00 | 0.00 |
| | | *Gastropod Larva* | | | 0.22 | 0.05 | 0.06 | 0.00 | 0.57 |
| | | *Isopod* | | | 0.00 | 0.03 | 0.00 | 0.05 | 0.00 |
| | | *Mysid* | | | 0.00 | 0.00 | 0.05 | 0.00 | 0.00 |
| | | *Nauplius* | 14 | b | 70.53 | 21.96 | 0.77 | 12.92 | 7.27 |
| | | *Ostracod* | | | 0.19 | 0.27 | 0.03 | 0.12 | 0.20 |
| | | *Polychaeta* | | | 0.03 | 0.14 | 0.00 | 0.05 | 0.98 |
| | | *Polychaeta Larva* | | | 0.15 | 0.05 | 0.03 | 0.00 | 0.00 |
| | | *Pteropod* | | | 0.00 | 0.00 | 0.00 | 0.00 | 0.12 |
| | | *Siphonophore* | | | 0.09 | 0.09 | 0.10 | 0.18 | 0.32 |
| | | *Unidentified* | | | 2.75 | 1.88 | 0.34 | 0.35 | 0.20 |
| | | *Zoea* | | | 0.45 | 0.09 | 0.00 | 0.05 | 0.96 |

Table 3 shows several Diversity Indices and Taxonomic Richness (applied to the taxonomic groups) for each station for the first 100m. Observing all the indices it is clear that Station 2 holds the highest biodiversity out of all the stations, for taxa considered in the first 100m. Taxonimic Richness is higher in Stations 1, 2, and 4 with 36, 32, and 33 taxa, respectively, while Stations 3 contains 24 taxa and Station 5 contains 29 taxa.

*Table 3: Diversity Indices and Species Richness for each station over the first 100m*

| Index | Stations | | | | |
| --- | --- | --- | --- | --- | --- |
| | 1 | 2 | 3 | 4 | 5 |
| Shannon H' Log Base 10, | 1.046 | 0.557 | 0.98 | 0.94 | 1.035 |
| Shannon Hmax Log Base 10, | 1.556 | 1.505 | 1.38 | 1.519 | 1.462 |
| Shannon J' | 0.672 | 0.37 | 0.71 | 0.619 | 0.708 |
| Simpsons Diversity (D) | 0.126 | 0.464 | 0.154 | 0.15 | 0.166 |
| Simpsons Diversity (1/D) | 7.956 | 2.157 | 6.485 | 6.661 | 6.026 |
| Taxonomic Richness | 36 | 32 | 24 | 33 | 29 |

**Identifying Cold and Warm Stations**

As seen earlier in Figure 6, the CTD data sheds some light on the thermal characteristics of each station. Figure 13 uses combined CTD/XBT data to produce a color contour plot of temperature in a cross-section along TZ and additional data, shown by the black isotherms, acquired by the undulating CTD (Fishscan), along T1, two days prior to the CTD/XBT deployment and biological sampling. Arrows indicate the stations' location and it can observed that, at the time of the sampling, Station 1 and 4 were located within a core of cold water while Station 2 sat on the margin of a cold core. In contrast, Stations 3 and 5 exhibit opposing thermal characteristics showing warmer temperatures. Comparing the measurements taken two days apart it is possible to observe a shift in the location of both cold cores.

For all further discussions the cold core to the north that includes Station 1, and marginally Station 2, is referred to as *Core A*; and the cold core to the south that includes Station 4, *Core B*. By observing the measurements from the two time points it appears that Core A is shifting northwards and Core B is moving southwards.
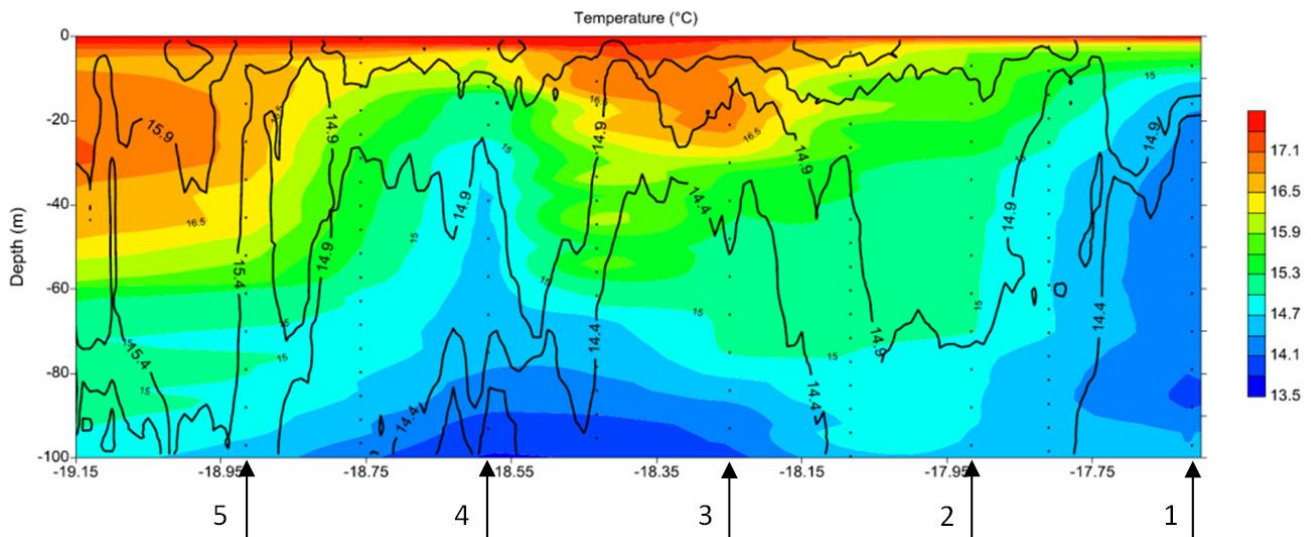
*Figure 13: Combined temperature map of undulating Fishscan data (black line isotherms) collected along T1 (1ˢᵗ October) and CTD/XBT data (colour contours) collected along the TZ (1ˢᵗ-3ʳᵈ October) (Muller et al., n.d.).*

**Taxonomic Composition Variation between Stations**

Beyond the taxonomic composition of each station described above, further analyses were performed to assess whether a taxonomic difference exists between stations and if so, what taxa is driving those changes. Since the difference in temperature between stations was negligible after 100m depth, these analyses were conducted on the taxonomic composition within the first 100m. The Principal Components Analysis (PCA) is shown in Figure 14 and the eigenvalues are presented in Table 4. Furthermore, Stations 1, 2 and 4 were labeled "cold" stations, while Stations 3 and 5 were labeled "warm" stations based on the CTD data discussed above. The graphical display of the PCA show us clear differences between the group of cold stations and the group of warm stations. These differences are reflected in PC1 which accounts for 51.5% of the variation (Table 4Table 5). Table 5 shows that the taxonomic groups driving the differences between the cold and warm stations are 'Fish egg', 'Unidentified Copepod I' and 'Nauplius'. In PC2 (27.8%) differences between stations, particularly, those between Station 2 compared with Stations 1 and 4, are motivated by *Oncaea spp*, *Metridia lucens*, and *C. carinatus copepodid*. PC3 shows differences between Stations 1 and 5, and Stations 2, 3, and 4. These differences are due to the abundances of "*Eucalanus hyalinus*", "Unidentified Copepod III" and 'Fish Egg'. The cumulative percentage of variation explained by these three principal components is over 93%.
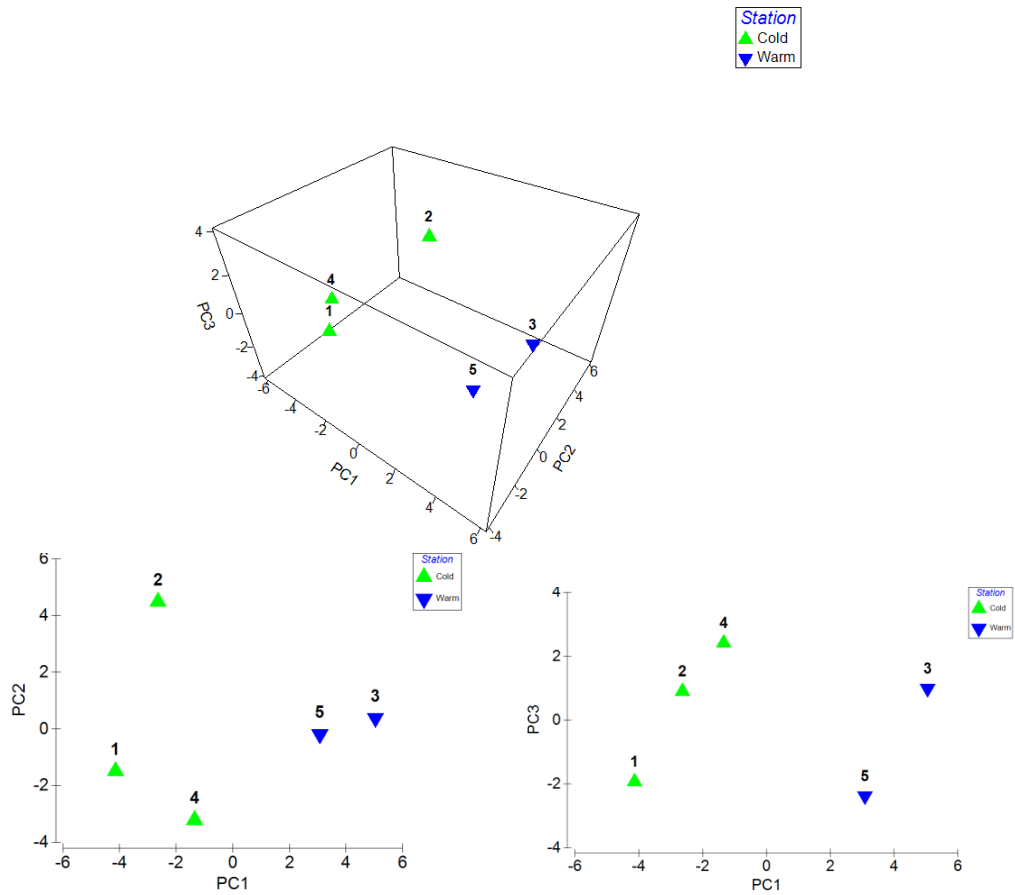
Figure 14: PCA, 3D on top and 2D below: PC1 vs PC2 on the left and PC1 vs PC3 on the right.

Table 4: Eigen values for PCA

| PC | Eigenvalues | %Variation | Cum.%Variation |
|---|---|---|---|
| 1 | 15,2 | 51,5 | 51,5 |
| 2 | 8,2 | 27,8 | 79,3 |
| 3 | 4,24 | 14,4 | 93,7 |
| 4 | 1,86 | 6,3 | 100 |

Table 5: PCA Results

| PC1 | | PC2 | | PC3 | |
|---|---|---|---|---|---|
| *Fishegg* | -0.529 | *Oncaea spp* | -0.458 | *Eucalanus hyalinus* | -0,413 |
| *Unidentified Copepod I* | -0.344 | *Metridia lucens* | -0.419 | *Unidentified Copepod III* | -0,378 |
| *Nauplius* | -0.339 | *C. carinatus copepodid* | 0.337 | *Fishegg* | 0,333 |
| *Metridia lucens* | -0.292 | *Calyptopis* | 0.309 | *Calanoides carinatus* | -0,301 |
| *Oncaea spp* | -0.263 | *Fishegg* | 0.297 | *Appendicularia* | -0,284 |
| *Acartia sp* | 0.185 | *Calanoides carinatus* | -0.250 | *Echinoderm Larva* | 0,229 |
| *Calyptopis* | -0.185 | *Centropages spp* | 0.211 | *Nauplius* | -0,206 |

| C. carinatus copepodid | -0.180 | Unidentified Copepod III | 0.207 | Chaetognath | -0,201 |
|---|---|---|---|---|---|
| Rhincalanus nasutus | -0.178 | Pleuromamma borealis | -0.175 | Acartia sp | 0,169 |
| Pleuromamma borealis | -0.177 | Echinoderm Larva | -0.168 | Zoea | -0,166 |
| .... | | | | | |

Figure 15 depicts the Bray Curtis similarity dendrogram between stations. Stations were classified as warm or cold as indicated. Here it can be observed that Stations 1 and 4 show the most resemblance, followed by the similarity of all three cold stations further demonstrating the existence of two distinct groups (cold and warm) and within the group of cold stations, two subgroups, those being inner-filament stations (1 and 4) and the marginal filament station (2).
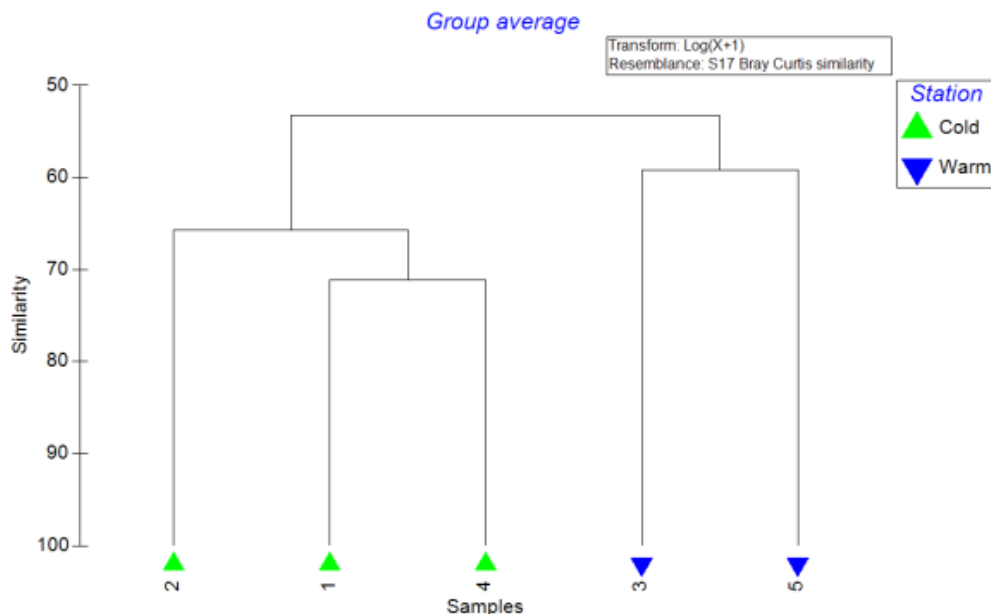


*Figure 15: Bray Curtis similarity dendrogram showing the similarity between stations*

Figure 16 shows the Dry Weight biomass per station for the first 100m depth. The values of DW biomass are 0.66, 1.57, 0.07, 0.38 and 0.17 g.m$^{-3}$ for stations 1, 2, 3, 4, and 5, respectively.
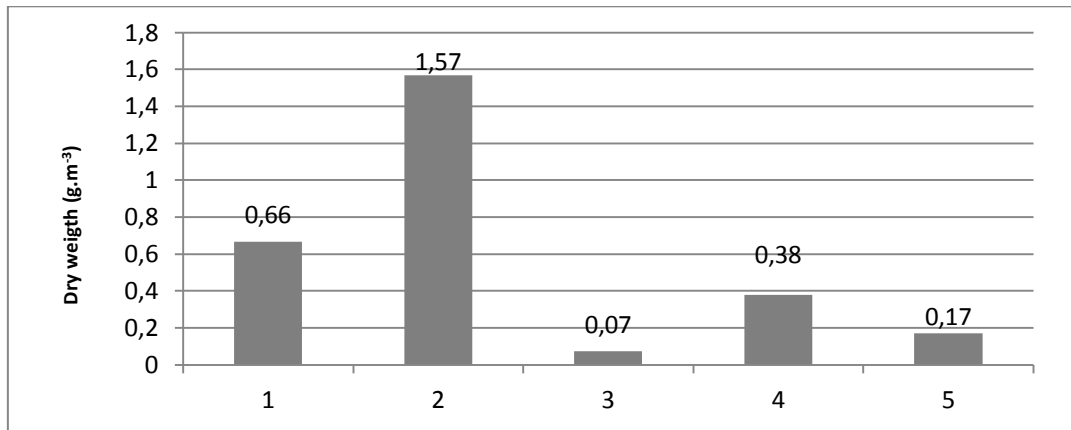
*Figure 16: Dry weight biomass per station in the first 100m*
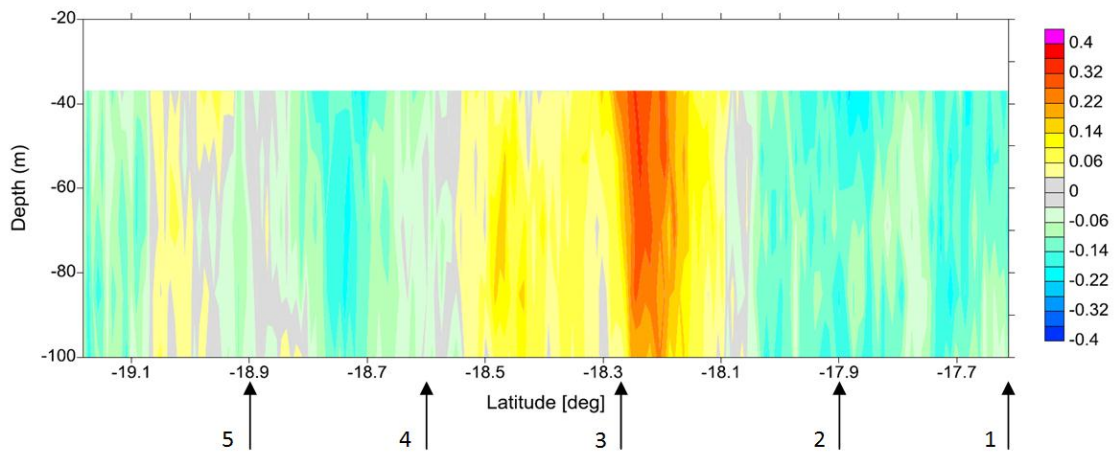


*Figure 17: ADCP current velocity*(Muller et al., n.d.)

*Table 6:Summary of current velocity and Biomass transport (positive = onshore; negative offshore)*

|  |  | Station | | | | |
|---|---|---|---|---|---|---|
|  | Depth | **1** | **2** | **3** | **4** | **5** |
| **ADCP current velocity** (m.s⁻¹) | 30 – 50 | -0,06 | -0,22 | 0,22 | -0,03 | 0 |
|  | 50 – 100 | -0,1 | -0,22 | 0,1 | -0,03 | -0,03 |
| **Biomass Transport** (µg.m⁻³)(m.s⁻¹) | 30 – 50 | -2588 | -36152 | 1138 | -769 | 0 |
|  | 50 - 100 | -3133 | -1857 | 81 | -283 | -10 |
|  | Total | -5721 | -38009 | 1219 | -1053 | -10 |

In Figure 17 is shown the current velocity and direction calculated with ADCP data, the arrows represent the stations. It is observed that the largest biomass transport is in Station 2 followed by Station 1. Station 3 shows the only onshore biomass transport. Station 4 has similar values of transport, although in the opposite direction. In Station 5 current velocity is close to zero, biomass is much reduced too, so the transport is almost null.

**Stable Isotope Analysis**

Isotopic analysis is presented in Figure 18. Trophic level (TL) is calculated based on 15N/14N [‰] scaled on either side of the graph. The x-axis represents 13C/12C [‰]. The species with highest TL is *Gaetanus sp.* (TL = 4) and *Paraeuchaeta hanseni* C4 (TL = 4) while both individuals of species *Tomopteris sp.* have the lowest TL (1.88; 2.03). All species are contained in values of 13C/12C [‰] ranging from -17.10 to -23.80 except for *Eucalanus hyalinus* with a value of -29.10.
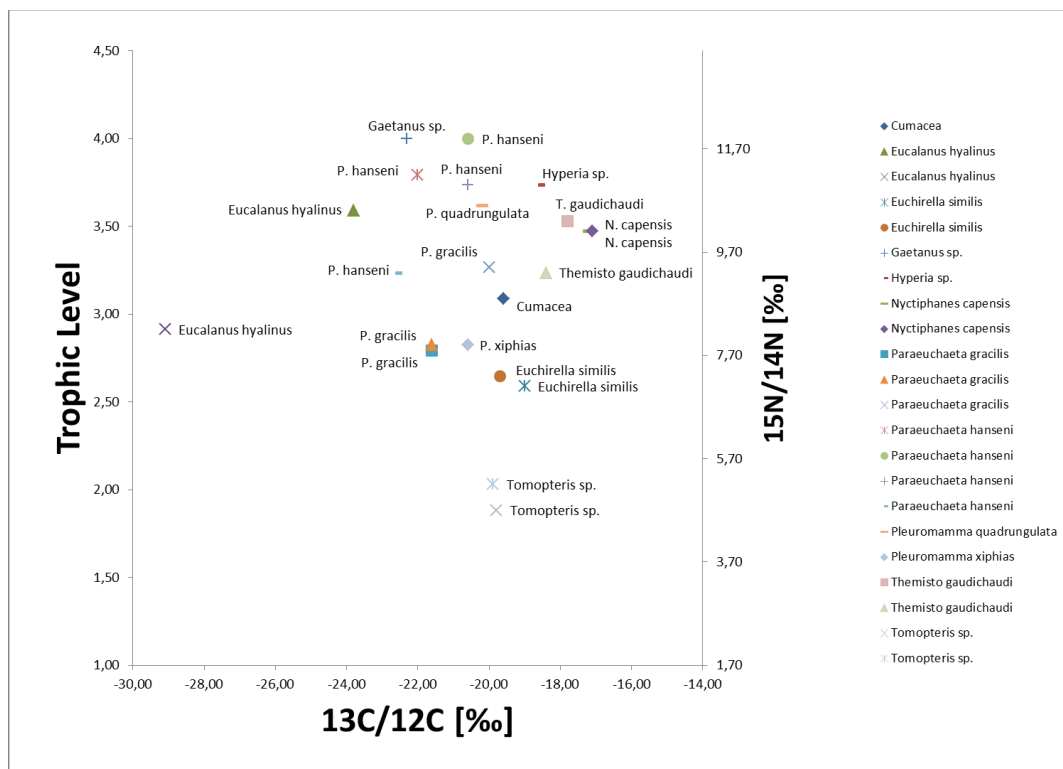


*Figure 18: Stable Isotope Analysis*

# 4. Discussion

Vertical profiles of temperature plotted from undulating CTD in transect 1 and 2 show a clear body of water colder than its surroundings. The two transects are 140km and 3 days apart, which indicates that this body of water was persistent for at least for this time and space frame. The temperature profiles also allowed for measurements of depth and width of the cold core of 100m and 38km, respectively. The dimensions describe a narrow body of water that developed more than 50km away from the generating upwelling front and had a length/width ratio higher than 2, consistent with the description of an upwelling filament proposed by (Kostianoy & Zatsepin, 1996). In addition, temperature profiles from transect 1 and CTD/XBT (taken 2 days after Scanfish) show a second core of cold water moving northwards. This second core captured in the temperature profiles of Transect 1 and CTD/XBT was not captured on Transect 2 nor sampled further. Filaments have been described to end in eddy-like features (Lutjeharms et al., 1991) but in this case, the end of the filament was recorded 140km away in the second transect. There were insufficient satellite images to accompany the development of the filament due to extensive cloud coverage so the body of water corresponding to the second core could not be followed through. We are left to speculate that either the filament split into two different cores or there were two filaments initially protruding from the upwelling front only 60km apart from each other, which appears to be less likely.

Measurements in situ were determinant for revealing the structure of the temperature profiles. Particularly, the combined CTD/XBT plots and the undulating CTD (Fishscan) proved to have enough spatial resolution to adequately assess the filament's structure and they both showed the same water bodies. Additionally, as the undulating CTD (Fishscan) and the CTD/XBT samples were taken 2 days apart, it provided an insight on the latitudinal movement of the upwelling. Discrete CTD measurements taken at the same time as MultiNet samples did not show enough horizontal resolution to visualize the filament. In figure 2 the SST map shows a protrusion of cold water that can hardly be classified as an upwelling filament. The stations are too spread apart and observed differences in temperature may be due to interpolation artifacts. However, the vertical resolution of the CTD allowed for the observation of temperature anomalies which permitted to classify MultiNet stations as cold or warm. Temperature profiles in figure 3 showed different characteristics of

the stations. The reference station N is consistent with the Angola Benguela Front with warm surface temperature (20°C) followed by a sharp thermocline. Profiles of the stations 1, 2, and 4 may be classified as those of an upwelling filament: a very weak and shallow thermocline, probably due to warming of the cold filament by the sun at the first 10 to 20m followed by steady cold temperatures, that of the filament core, until the end of the vertical width of the filament when temperatures decline again in synchrony with all the temperature profiles. Stations 3, 5, and reference station to the south S, are warmer at the surface than the remaining profiles and appear to register incursions of different water masses with profile 3 presenting two thermoclines at 25m down to the same temperature as profile 2 and then again at 80m where all profiles converge. In contrast, profile from station S exhibits an incursion of warm water. Thus, the temperature profiles seem to be adequate to identify an upwelling filaments as the shape of the profiles in stations 1, 2, and, 4 are fairly similar and the position of the sampling stations is coherent with the two filament cores identified in CTD/XBT section profiles. The sampling strategy adopted of using one initial satellite image to identify the location of the developing stage of an upwelling filament proofed certain as the filament was indeed captured; still the initial classification of the stations had to be adapted. The latitudinal movement of the upwelling filament forced a reclassification of the MultiNet sampling stations based on the oceanographic characteristics observed on site. Stations 1 and 4 were in fact inside the two cores of the filament, station 2 was located in the boundary of Core 1 and Station 3 and 5 were outside of the filament's cores.

Vertical distribution of zooplankton revealed a pattern specific to each group of stations. This can be observed in Figure 12, stations belonging to the filament showed very high abundances in the surface layer of the water column, which decreased successively down the lower strata of the water column. As the large percentage of taxonomic groups is herbivore and the stratum close to the surface is known to hold the highest biomass of phytoplankton, it is obvious why zooplankton reaches higher abundances at the surface. This is coherent with previous observations for faunal abundances in filaments (Shillington et al., 1990). Similarly, as phytoplankton biomass decays and sinks in the water column (Helly & Levin, 2004), it becomes less available for zooplankton to graze on, explaining the low abundances found in the deeper layers sampled. No trends were found relating the

time of sampling with the depth at which the highest abundance of copepods was found. A possible explanation for this is that copepods remain feeding in the upper layers of the water column. Behavioral changes have been observed in copepods in relation to water temperature and dissolved oxygen. In a study of hypoxia tolerance, it was observed that copepods reduced their diel migration to the first 60 m avoiding the intermediate oxygen minimum layer (Auel & Verheye, 2007). It may be speculated that copepods may interrupt or restrain their diel migration to feed as much as possible in the shortest amount of time, before resuming extensive diel migrations again.

As seen above, there is strong evidence for two distinct sets of stations, cold stations, those being within the upwelling filament, and warm, those of the adjacent waters. The abundances of zooplankton followed the same pattern showing elevated abundances in cold stations compared to the warm stations. This fact supports the hypothesis that there is higher abundance within the upwelling filament waters than in the warm tropical waters. Regardless of the fish eggs' extremely high abundance in the surface waters located in the margin of the filament, another taxon, Unidentified Calanoids, revealed very high abundances that were transversal to both bodies of water sampled. Due to time constrains and dimension of the individuals, this taxon could not be identified to species level but this group was composed by small calanoids, probably herbivores. These, are known to be widely distributed over the Benguela System. Still, the fact that this taxon was present in high number in all stations, though more abundant inside the filament, indicates that it does not contribute for a different taxonomic composition between the filament and the tropical ocean. There were few groups with the same order of magnitude of abundance for all stations. Besides the supra mentioned "Unidentified Calanoids", groups *Heterorhabdus spp*, *Pleuromamma borealis*, *Oithona spp.* and Chaetognaths also presented similar abundances through the different stations. *Oithona spp.* is known to be one of the most ubiquitous and abundant genera amongst the copepods (Gallienne, 2001). The numbers of *Oithona spp* shown here are not very high, the abundance of *Oithona spp* is probably underestimated as this genus is smaller than the mesh size used in the plankton nets. *Sagitta friderici* has been described as the most common species of chaetognaths in the Benguela system (Gibbons, 1994) (Gibbons 1994), however another study reports *Sagitta setosa* as he most abundant

chaetognath (>70%)(Duro & Gili, 1996). The two species are reportedly difficult to tell apart, yet both species are known to be neritic and typical of upwelled waters which may account for the abundances inside the filament. The reason for being equally abundant in the warm waters outside the filament is probably because it concerns another species.

Taxonomic groups with different abundances inside and outside the filament were highlighted by the PCA. PCA proved to be a good analytical tool to assess the different taxonomical groups in each set of stations. "Unidentified Copepod I" consists of a group of small calanoids, most likely herbivore, which was mostly found inside the filament's waters. Empirical observation in this study showed that diatom-dominated samples were found in stations 1 and 2, inside the filament, which may account for the large numbers of herbivore copepods that were drawn offshore by the filament while grazing on phytoplankton (Batten & Fileman, 2001). In fact, the numerous herbivore copepods was not the only taxon found to have higher abundances inside the filament, PC1 also identifies Nauplius as one of the taxa promoting the differences between the two groups of stations.

*Metridia Lucens*, an omnivore copepod, was also found in higher number inside the filament's core as pointed in PC1. Further evidence for differences in taxonomic composition between the core of the filament and its margin was given by PC2. PC2 shows that Stations 1 and 4, those belonging to the filament's core, differ in their composition due to the abundances of *Oncaea spp* and *Metridia Lucens*, while *C. carinatus* copepodid, Calyptopis and Fish egg are more characteristic of the filament's margin sampled in station 2. Further analysis of the vertical distribution of these latter groups shows that these three groups were found at the surface. Plausible explanations for this fact may reside in the fact these particles have neutral buoyancy which combined with the offshore movement inside the filament versus the onshore movement of the adjacent waters, may concentrate these organisms in the boundary areas of the filament. Indeed, concentration of particles is known to occur in convergent bodies of water (Agustini & Bakun, 2002)

Empirical observations during the course of this study permit to draw some remarks on whether the samples were diatom-dominated (circa 100000 particles per m$^3$) or dinoflagellate-dominated and its relation to either the warm groups of stations or the

cold ones. As expected, diatom-dominated samples were located in cold stations as opposed to dinoflagellates which dominated warm stations. Though neither of these groups was quantified, others typical of the warm tropical ocean were. Examples include Siphonophores, Medusae and Appendicularia found mostly, and in the case of Appendicularia, exclusively in warm stations. Typical of non-copepod fauna of the oligotrophic Southeast-Atlantic (Gibbons, Gugushe, & Boyd, 1999).

Impacts on recruitment

The Benguela system gathers the conditions necessary for fish stock development to reach high biomass when the so called triad of enrichment, retention and concentration reaches an optimum (Bakun 1996, Hutchings 2002). Of course not only fish depends on retention for successful development, besides fish eggs and larvae, other early stage organisms like calyptopis, nauplius, copepodids depend on coastal retention. These latter ones are further subjected to concentration due to convergence currents (Shelton and Hutchings 1990). In this study it has been established that filament carry high abundances of zooplankton. Specifically, it has been seen in the PCA and vertical distribution table that taxonomic groups *C. carinatus* copepodid, Caplyptopis, Nauplius, Fish eggs and Fish larvae show very high abundance within the filament. Furthermore, in the Northern Benguela subsystem, particles within the first 40 m are known to drift offshore via Ekman transport (Verfaillie, Degraer, Schelfaut, Willems, & Van Lancker, 2009)(Stenevik, Skogen, & Sundby, 2003). The same offshore transport of biomass was found in the upwelling filament under study here (see below) and the offshore transport associated with this structure was more than double of the integrated Ekman transport in this study area(Muller et al. under submission for publication). In addition, the total of transport carried by filaments in the Benguela System constitutes half of all Ekman transport, resulting in an export of particles from the coast to the oligotrophic ocean (Kostianoy & Zatsepin, 1996). Considering that organisms transported offshore will not reach their full development , all the before mentioned factors combined point to not only a very high impact of filaments on the advective loss of spawned organisms inshore, but also to a potential important food source for pelagic species offshore.

ADCP data provided a very good insight of the current dynamics in the section sampled (Muller et al. under submission for publication). In fact, the ADCP, CTD/XBT and MultiNet taken all in the same transect allowed for a match between currents, temperature and zooplankton abundance. This combination of data permitted to pinpoint the exact location of the filament, its velocity and direction, and the biomass associated with each body of water.  The calculation of biomass transport given by the product of biomass and velocity may not robust enough to accurately quantify the biomass transport of the filament, and the one of its reflux, but it provides evidence for offshore transport of biomass carried by the filament.

Despite being collected onshore and offshore on a coastal upwelling zone, Stable isotopes samples were not taken during an upwelling filament event. In addition, the amount of copepods collected onshore was too scarce to allow any comparisons on trophic level changes inshore and onshore. Nevertheless, the study of stable isotopes along an upwelling filament would certainly be adequate to evaluate whether organisms simply drift away from shore or graze and predate while transported by the filament. It has been shown, for instance, that copepod egg production is increased inside the filament (Smith & Lane, 1991).

# 5. Conclusions

The cold stations identified with the upwelling filament are characterized by very high abundances and biomass, and also increased diversity. In contrast, the warm waters surrounding the filament show a much reduced biomass, abundance and number of taxonomic groups. Vertical distribution of copepods may point to changes in the range of diel migration. Upwelling filaments represent half of the Ekman transport leading to a strong export of biomass into the oligotrophic ocean. Further implications of this transport need, therefore, to better investigated. Similarly, the trophic dynamics inside the filament are unclear. As the frequency of the upwelling filaments may be affected by climate change, it is crucial to continue to study the role of upwelling filaments in the biogeochemical cycle.

# 6. References

Alvarez-Salgado, X., Doval, M., Borges, A., Joint, I., Frankignoulle, M., E.M.S., W., & Figueiras, F. G. (2001). Off-shelf fluxes of labile materials by an upwelling filament in the NW Iberian upwelling system. *Progress In Oceanography*, *51*, 321-337. Retrieved from http://www.sciencedirect.com/science/article/pii/S0079661101000738

Auel, H., & Verheye, H. (2007). Hypoxia tolerance in the copepod Calanoides carinatus and the effect of an intermediate oxygen minimum layer on copepod vertical distribution in the northern Benguela Current upwelling system and the Angola–Benguela Front. *Journal of Experimental Marine Biology and Ecology*, *352*(1), 234-243. doi:10.1016/j.jembe.2007.07.020

Batten, S., & Fileman, E. (2001). The contribution of microzooplankton to the diet of mesozooplankton in an upwelling filament off the north west coast of Spain. *Progress in oceanography*, *51*, 385-398. Retrieved from http://www.sciencedirect.com/science/article/pii/S0079661101000763

Brink, K. (1983). The near-surface dynamics of coastal upwelling. *Progress in Oceanography*, *12*, 223-257. Retrieved from http://www.sciencedirect.com/science/article/pii/0079661183900095

Clarke, K. R., & Warwick, R. M. (1994). Change in Marine Communities: An Approach to Statistical Analysis and Interpretation. *Natural Environment Research Council* (p. 144).

Duro, A., & Gili, J.-maria. (1996). Mesoscale spatial heterogeneity in chaetognath populations during upwelling abatement in the northern Benguela region, *140*, 41-58.

Flament, P., & Washburn, L. (1985). The Evolving Structure of an Upwelling Filament. *JOURNAL OF GEOPHYSICAL RESEARCH*, *90*.

Gallienne, C. (2001). Is Oithona the most important copepod in the world's oceans? *Journal of Plankton Research*. Retrieved from http://plankt.oxfordjournals.org/content/23/12/1421.short

Gibbons, M. (1994). Diel vertical migration and feeding of Sagitta friderici and Sagitta tasmanica in the southern Benguela upwelling region, with a comment on the on the structure of the guild of primary carnivores. *Marine ecology progress series*, *111*(Heydorn 1959), 225-240. Retrieved from http://www.int-res.com/articles/meps/111/m111p225.pdf

Gibbons, M., Gugushe, N., & Boyd, A. (1999). Changes in the composition of the non-copepod zooplankton assemblage in St Helena Bay (southern Benguela ecosystem) during a six day drogue study. *Marine Ecology*, *180*, 111-120. Retrieved from http://www.int-res.com/abstracts/meps/v180/p111-120/

Haynes, R., Barton, E. D., & Lino, I. P. R. (1993). Development , Persistence , and Variability of Upwelling Filaments off the Ariantic Coast of the Iberian Peninsula, *98*(93).

Helly, J. J., & Levin, L. a. (2004). Global distribution of naturally occurring marine hypoxia on continental margins. *Deep Sea Research Part I: Oceanographic Research Papers*, *51*(9), 1159-1168. doi:10.1016/j.dsr.2004.03.009

Hernández-León, S., Gómez, M., & Arístegui, J. (2007). Mesozooplankton in the Canary Current System: The coastal–ocean transition zone. *Progress In Oceanography*, *74*(2-3), 397-421. doi:10.1016/j.pocean.2007.04.010

Huggett, J., Verheye, H., Escribano, R., & Fairweather, T. (2009). Copepod biomass, size composition and production in the Southern Benguela: Spatio–temporal patterns of variation, and comparison with other eastern boundary upwelling systems. *Progress In Oceanography*, *83*(1-4), 197-207. Elsevier Ltd. doi:10.1016/j.pocean.2009.07.048

Hutchings, L., van der Lingen, C. D., Shannon, L. J., Crawford, R. J. M., Verheye, H. M. S., Bartholomae, C. H., van der Plas, a. K., et al. (2009). The Benguela Current: An ecosystem of four components. *Progress In Oceanography*, *83*(1-4), 15-32. Elsevier Ltd. doi:10.1016/j.pocean.2009.07.046

Keister, J. E., Cowles, T. J., Peterson, W. T., & Morgan, C. a. (2009). Do upwelling filaments result in predictable biological distributions in coastal upwelling ecosystems? *Progress In Oceanography*, *83*(1-4), 303-313. Elsevier Ltd. doi:10.1016/j.pocean.2009.07.042

Keister, J. E., Di Lorenzo, E., Morgan, C. a., Combes, V., & Peterson, W. T. (2011). Zooplankton species composition is linked to ocean transport in the Northern California Current. *Global Change Biology*, *17*(7), 2498-2511. doi:10.1111/j.1365-2486.2010.02383.x

Kostianoy, A. G., & Zatsepin, A. G. (1996). The West African coastal upwelling filaments and cross-frontal water exchange conditioned by them. *Journal of Marine Systems*, *7*(2-4), 349-359. doi:10.1016/0924-7963(95)00029-1

Loick, N., & Ekau, W. (2005). Water-body preferences of dominant calanoid copepod species in the Angola-Benguela frontal zone. *African Journal of Marine Science*, (March 2012), 37-41. Retrieved from http://www.tandfonline.com/doi/abs/10.2989/18142320509504120

Lutjeharms, J. R., Shillington, F. a, & Rae, C. M. (1991). Observations of extreme upwelling filaments in the southeast atlantic ocean. *Science (New York, N.Y.)*, *253*(5021), 774-6. doi:10.1126/science.253.5021.774

MOTODA, S. (1959). Devices of simple plankton apparatus. *Memoirs of the Faculty of Fisheries*. Retrieved from http://eprints2008.lib.hokudai.ac.jp/dspace/handle/2115/21829

Muller, A. A., Mohrholz, V., & Schmidt, M. (n.d.). Quantifying the offshore transport associated with a northern Benguela upwelling filament 1 during October 2010. *Under submission for publication*.

Nelson, G., Boyd, A., & Agenbag, J. (1998). An upwelling filament north-west of Cape Town, South Africa. *South African Journal of*, (June 2012), 37-41. Retrieved from http://www.tandfonline.com/doi/abs/10.2989/025776198784126953

Pauly, D., & Christensen, V. (1995). Primary production required to sustain global fisheries. *Nature*, *374*(March), 255-257.

Rodriguez, J., Hernandezleon, S., & Barton, E. (1999). Mesoscale distribution of fish larvae in relation to an upwelling filament off Northwest Africa. *Deep Sea Research Part I: Oceanographic Research Papers*, *46*(11), 1969-1984. doi:10.1016/S0967-0637(99)00036-9

Shannon, L., Boyd, A., & Brundrit, G. (1986). On the existence of an El Nino-type phenomenon in the Benguela System. *Journal of marine*. Retrieved from http://www.ingentaconnect.com/content/jmr/jmr/1986/00000044/00000003/art00005

Shannon, L. V., & O'Toole, M. (2003). Sustainability of the Benguela: ex Africa semper aliquid novi. *Large Marine Ecosystems of the World: Trends in Exploitation, Protection and Research*, 227-253. Retrieved from http://oceandocs.org/handle/1834/396

Shelton, P., & Hutchings, L. (1990). Ocean stability and anchovy spawning in the southern Benguela Current region. *Fishery Bulletin*, (Shelton 1986), 323-338. Retrieved from http://www.csa.com/partners/viewrecord.php?requester=gs&amp;collection=ENV&amp;recid=2313536

Shillington, F., Peterson, W., Hutchings, L., PROBYN, T. A., WALDRON, H. N., & AGENBAGI, J. J. (1990). A cool upwelling filament off Namibia, southwest Africa: preliminary measurements of physical and biological features. *Deep Sea Research*, *37*(I), 1753-1772. Retrieved from http://www.sciencedirect.com/science/article/pii/0198014990900757

Smith, S. L., & Lane, P. V. Z. (1991). The Jet off Point Arena, California: Its Role in Aspects of Secondary Production in the Copepod Eucalanus californicus Johnson. *JOURNAL OF GEOPHYSICAL RESEARCH*, *96*(C8), 14849–14858.

Stenevik, E., Skogen, M., & Sundby, S. (2003). The effect of vertical and horizontal distribution on retention of sardine ( Sardinops sagax ) larvae in the Northern Benguela – observations and modelling. *Fisheries*, (July 2001), 185-200. Retrieved from http://onlinelibrary.wiley.com/doi/10.1046/j.1365-2419.2003.00234.x/full

Strub, P., Kosro, P., & Huyer, A. (1991). The nature of the cold filaments in the California Current System. *JOURNAL OF GEOPHYSICAL RESEARCH*, *96*, 14743-14768. Retrieved from http://scholar.google.com/scholar?hl=en&btnG=Search&q=intitle:The+Nature+of +the+Cold+Filaments+in+the+California+Current+System#0

Traganza, E. D., Conrad, J. C., & Breaker, L. C. (1981). Satellite observations of a cyclonic upwelling system and giant plume in the California Current. *Coastal coastal estuarine sciences*, *1*, 228 - 241.

Troupin, C, Machín, F., Ouberdous, M., Sirjacobs, D., Barth, A., & Beckers, J.-M. (2010). High-resolution climatology of the northeast Atlantic using Data-Interpolating Variational Analysis (Diva). *Journal of Geophysical Research*, *C8*(115), 1-20.

Troupin, Charles, Mason, E., Beckers, J.-M., & Sangrà, P. (2012). Generation of the Cape Ghir upwelling filament: A numerical study. *Ocean Modelling*, *41*, 1-15. Elsevier Ltd. doi:10.1016/j.ocemod.2011.09.001

Verfaillie, E., Degraer, S., Schelfaut, K., Willems, W., & Van Lancker, V. (2009). A protocol for classifying ecologically relevant marine zones, a statistical approach. *Estuarine, Coastal and Shelf Science*, *83*(2), 175-185. Elsevier Ltd. doi:10.1016/j.ecss.2009.03.003

## Acknowledgments